AUTOPILOT DESIGN DOR THE LATERAL-DIRECTIONAL MOTION OF AN UAV

Costin ENE, Adrian-Mihail STOICA, Petrisor-Valentin PARVU

University "Politehnica" of Bucharest, Faculty of Aerospace Engineering, Bucharest, Romania (ene.costin27@gmail.com, adrian.stoica@upb.ro, parvupv@gmail.com)

DOI: 10.19062/2247-3173.2017.19.1.43

Abstract: *The aim of the paper is to present a design procedure for the lateral-directional autopilot of an unmanned aerial vehicle (UAV) using a modified loop-shaping based control configuration. The design objectives include besides robust stability properties, the tracking of a reference model chosen such that maneuverability performances are accomplished. A reduced order autopilot is obtained solving an H_∞ norm minimization problem with imposed structure of the controller. The proposed design methodology is illustrated and validated by a case study in which the performances of the lateral autopilot are analyzed for various flight conditions.*

Keywords: *UAV, Lateral-Directional dynamics, loop shaping, robust stability, ideal model tracking, H_∞ norm minimization, Hinfstruct*

1. INTRODUCTION

Unmanned Air Vehicle's (UAV's) are widely used in several domains of activity including the military domain. Some of the advantages for these types of aircraft are that their structure is usually of small dimensions, which makes them light, have great autonomy and able to reach places that pose danger for humans. They can also be used in reconnaissance or surveillance missions. There exist several types of UAV from which the flying wing configuration has the main advantage of having reduced drag and energy consumption. A drawback of these types of UAV is that their dynamics are usually unstable, thus they require automatic control in order to obtain the desired maneuverability qualities. In order to ensure stability several control techniques have been proposed in the available literature such as PID control [1], dynamic inversion and μ-Synthesis [2], LQR and LQG control [3,4], L_1 norm based techniques [5], H_∞ norm minimization [7]. All these methods require ensuring a trade-off between their achievable performance and the robustness requirements. The actual applications require a wide spectrum of performances including not only the stabilization of the aircraft but also robustness with respect to modeling uncertainties and flying conditions changes, time response performances and reduced sensitivity to disturbances and measurement errors. H_∞ control theory is well suitable to handle control design specifications and create an environment that allows for systematic handling of performance and robustness objectives. Practice, however, shows that numerical issues can arise when dealing with flexible and high dimensional control problems. The resulting controllers from the synthesis procedure usually have a high order because H_∞ design is a full-order method which provides controllers of the same order as the weighted synthesis model which is the sum of the order of the controlled plant and the order of the used weightings.

Also different hardware or software constrains (given by the computational power for example) can impose post-design truncation procedures in order to reduce the controller dimension.

The aim of this paper is to present a reduced order H_∞ design based on structured μ-Synthesis developed in [8] for the Heading Hold (HH) autopilot of the flying wing configuration Hirrus UAV. This UAV was designed and manufactured by a private Romanian company in collaboration with academics from Faculty of Aerospace Engineering of University "Politehnica" of Bucharest. In [7] the design approach is based on a modified version of the so-called two degrees of freedom (2 DOF) H_∞ loop-shaping and it`s able to accomplish simultaneously several objectives as robustness stability, model tracking and disturbances attenuation requirements. A comparison between the full order controller and the reduced order controller obtained through truncation using a balanced realization procedure [7] and the reduced order controller using structured μ-Synthesis is provided.

The paper is organized as follows: in the second section, the design objectives, the design model of the UAV and the Simulink model of the heading hold autopilot are presented. The third section provides some insight on the structured μ-Synthesis controllers, but more details can be found in [8]. Simulation results, for the Hirrus UAV, that include atmosphere turbulences are provided in section four as a comparison between three controllers: the full eight-order controller and its truncated fifth-order version obtained in [7] and the structured μ-Synthesis controller which is only second-order. The paper ends with some concluding remarks.

2. DESIGN MODELS AND AUTOPILOT SYNTHESIS OBJECTIVES

The Hirrus platform illustrated in Fig. 1 has a flying wing configuration with the wingspan 3.2 m, length 1.2 m, maximum takeoff weight 6.5 kg, maximum cruising speed of 80 km/h and with a maximum payload of 1 kg.

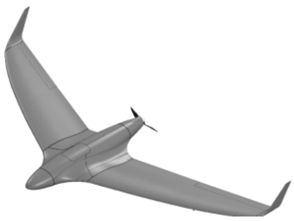

FIG.1. Hirrus UAV [6]

The lateral-directional dynamics of the UAV is approximated by the following linearized nominal model:

$$\begin{aligned}\dot{x}(t) &= Ax(t) + B\delta(t)\\ y(t) &= Cx(t) + D\delta(t),\end{aligned} \tag{1}$$

where $x(t) = [v(t); p(t); r(t);\ \phi(t);\ \psi(t)]$ is the state vector with components sideslip velocity v, roll rate p, yaw rate r, roll angle ϕ and the heading angle ψ respectively. The control input $\delta(t)$ denotes the elevon deflection, while $y(t) = [r(t);\ \phi(t);\ \psi(t)]$ denote the measured outputs. For the nominal flight conditions $V = 14.8277\ m/s$ and the cruising altitude $h = 1000\ m$, the state matrix A, the control matrix B and the output matrices C and D are given by:

$$A=\begin{bmatrix}-0.0742 & 0.1174 & -14.7871 & 9.81 & 0\\ -0.8443 & -19.2893 & 3.7078 & 0 & 0\\ 0.2689 & -1.1721 & -0.1960 & 0 & 0\\ 0 & 1 & 0 & 0 & 0\\ 0 & 0 & 1 & 0 & 0\end{bmatrix};B=\begin{bmatrix}0.1419\\ 8.6676\\ -0.3126\\ 0\\ 0\end{bmatrix};C=\begin{bmatrix}0&0&1&0&0\\0&0&0&1&0\\0&0&0&0&1\end{bmatrix};D=\begin{bmatrix}0\\0\\0\end{bmatrix}. \qquad (2)$$

The above flight condition is unstable in the absence of an automatic flight control system, fact which can be seen by computing the eigenvalues of the state matrix $\lambda_A=\{0;\,-19.1207;\,-0.2597\pm 2.2877i;\,0.0805\}$.

The design objectives for the HH autopilot are:

(DO1) Stabilization of the lateral-directional dynamics;

(DO2) Zero steady state value for the tracking error $\psi_{com}-\psi(t)$ for piecewise constant values of the commanded heading angle ψ_{com};

(DO3) Coordinated turns implying accomplishing the condition ([10])

$$r=\frac{g}{V}\tan(\phi); \qquad (3)$$

(DO4) Reduced sensitivity with respect to low frequency measurement errors and robust stability with respect to modeling uncertainties.

These design objectives are achieved using a 8-th order optimal H$_\infty$ controller. The controller architecture can be found in [7], where the authors also used a balanced realization technique in order to reduce the order of the controller from 8 to 5.

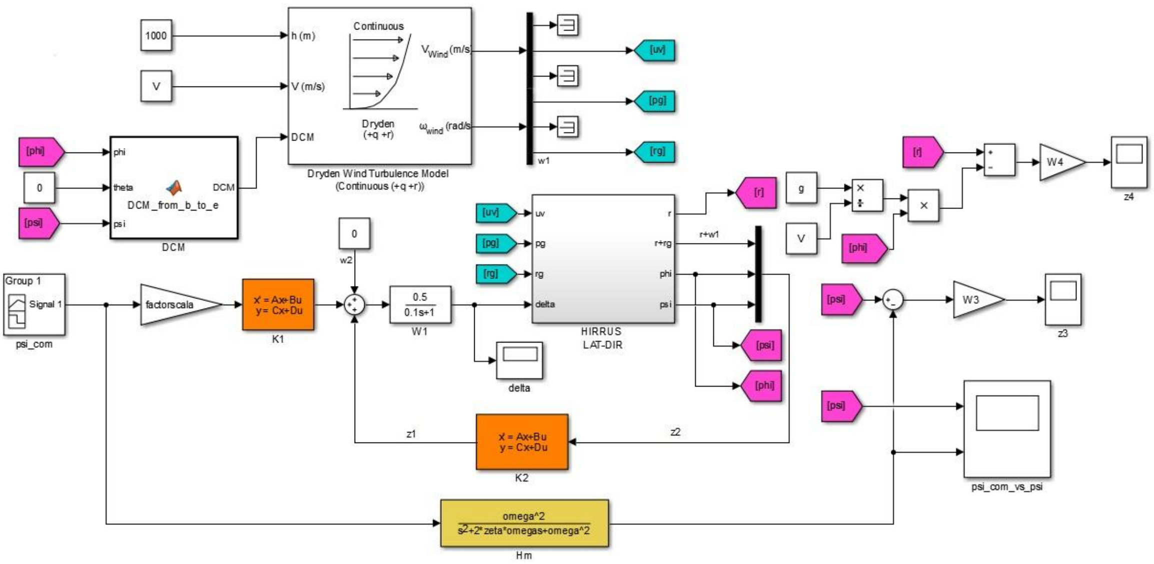

FIG.2. HIRRUS control configuration with 2DOF autopilot

In Fig.2 The control problem is finding $K=[K_1\;K_2]$ that stabilizes the system given by (1,2) and minimizes the H$_\infty$ norm of the mapping $u_1\rightarrow y_1$ where

$$u_1=\begin{bmatrix}\psi_{com}\\ w_1\\ w_2\end{bmatrix}\text{ and } y_1=\begin{bmatrix}z_1\\ z_2\\ z_3\\ z_4\end{bmatrix} \qquad (4)$$

In the above configuration the reference model H_m has $\omega_m=0.6\,rad/s$ and $\zeta_m=0.7$, $W_3=100$ and $W_4=10$.

The only modification is $W_1(s) = \frac{0.5}{0.1s+1}$ instead of the value $W_1(s) = \frac{100}{0.1s+1}$ used in [7] because if sensitivity is pushed down in the low frequency range (i.e, good load disturbance rejection and reference tracking), it increases by an equal amount at others frequencies amplifying for instance control command or noise propagation. Thus using 0.5 instead of 100 for W_1 will still keep the sensitivity acceptable for low frequency range disturbances while providing a reasonable values for the control input, the elevon deflection δ.

The aim of this paper is to replace the 8-th order controller $K = [K_1\ K_2]$ obtained in [7] with a reduced order one obtained using the structured μ-Synthesis design.

3. STRUCTURED - SYNTHESIS DESIGN

Consider the interconnected synthesis scheme of Fig. 3 where the weighting functions W_1, W_2, W_3 and W_4 are introduced to shape the closed loop system responses according to the robust performance and stability margin requirements. The trimmed plant dynamics is represented by $P_0(s)$. The uncertain system is modeled as $G(s) = P_0(s)(I + W_c(s)\Delta_c)$, where Δ_c belonging to some known set, represents the uncertain dynamics with unit peak gain and $W_c(s)$ is a stable, minimum-phase shaping filter that adjusts the amount of uncertainty at each frequency. One can notice that even though the problem formulation here is not exactly the same as in Fig. 2, it has some similarities. In Fig. 2 w_1 and w_2 represent the same type of additive uncertainties as d_1 and d_2. Also the case from Fig. 2 does not include the multiplicative uncertainties given by Δ_c and in Fig. 3 one doesn't use a reference model in order to shape the output y neighter split the controller K into two controllers K_1 and K_2. However, adjustments were made in order to solve the control problem form Fig. 2 using the μ-Synthesis design.

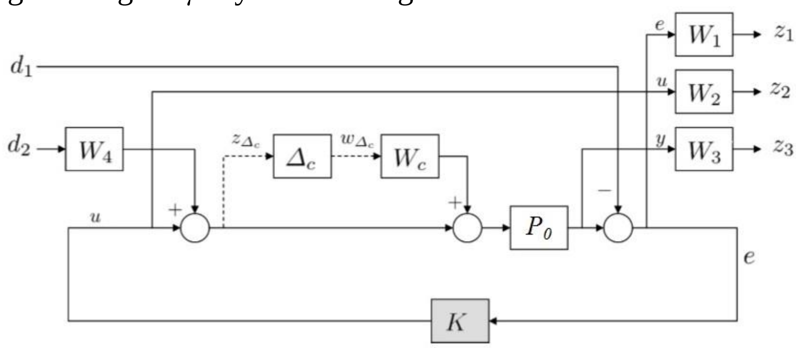

FIG.3. Closed loop interconnected structure of the μ-Synthesis design

This system in Fig. 3 can be rearranged as a generalized μ-Synthesis design as shown in Fig. 4. Considering the open loop interconnection $\tilde{P}$ (the partition matrix of *P*) one must find a stabilizing controller $K(s)$ such that the peak value μ_Δ of the closed loop transfer function $L(s) = F_l(\tilde{P}, K)$ is minimized:

$$\min_{K(s)} \max_\omega \mu_\Delta F_l\left(\tilde{P}(j\omega), K(j\omega)\right), \tag{5}$$

where $\Delta := diag(\Delta_c, \Delta_p)$. Δ_p is introduced to close the loops between the input and output channels associated to the performance criterion and $L(j\omega) = F_l\left(\tilde{P}(j\omega), K(j\omega)\right) = \tilde{P}_{11} + \tilde{P}_{12}K\left(I - \tilde{P}_{22}K\right)^{-1}\tilde{P}_{21}$.

Thus the resulting partitioned matrix $\tilde{L}_{ij}, (i,j) \coloneqq 1:2$ is given by:

$$\begin{bmatrix} z_{\Delta_c} \\ \hline z_1 \\ z_2 \\ z_3 \end{bmatrix} = W_a \left[\begin{array}{c|cc} -T & KS & S \\ \hline -GS & S & -GS \\ -T & KS & -T \\ GS & T & GS \end{array}\right] W_b \begin{bmatrix} \omega_{\Delta_c} \\ \hline d_1 \\ d_2 \end{bmatrix}, \tag{6}$$

where $S = (I + GK)^{-1}$ and $T = GK(I + GK)^{-1}$ denote the output sensitivity and the complementary sensitivity functions and $z_{\Delta_c} = \Delta_p \omega_{\Delta_c}$. The control design objectives are shaped by the weighting functions given by $W_a = diag(W_c, W_1, W_2, W_3)$ and $W_b = diag(I_2, W_4)$.

These filters are designed in order to limit the undesired effects of the off diagonal elements, thus resulting in a less conservative solution. Typos on how to tune these weighting functions can be found in [8].

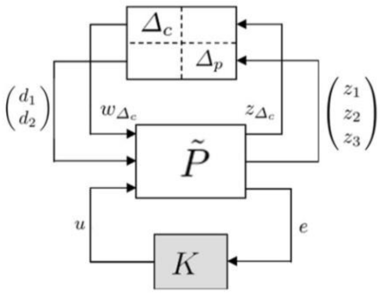

FIG.4. Closed loop interconnected design for the generalized μ-Synthesis

The main idea for obtaining a solution with reduced order is to approximate the μ-function by its upper bounds which remains an optimally scaled maximum singular value:

$$\mu_\Delta(L) \leq \inf_{D \in \Lambda} \bar{\sigma}\left(D \tilde{P} D^{-1}\right) \tag{7}$$

where D is the set of scaling matrices commuting with Δ and belonging to the set Λ

$$\Lambda = \{D = D^T > 0 : \ \forall \Delta, \Delta D = D\Delta\} \tag{8}$$

Thus the minimization problem in (5) is reformulated into

$$\min_{K(s)} \min_{D \in \Lambda} \left\| D(j\omega) F_l\left(\tilde{P}(j\omega), K(j\omega)\right) D^{-1}(j\omega) \right\|_\infty, \tag{9}$$

which can be solved using procedures from [9].

The structured μ-synthesis problem is formulated as a systematic Multi-Model control design problem. The control design objectives are decomposed into three main interconnection schemes that is *S*, *GS* and *GK*, in order to avoid interactions between control objectives. In the structured design those closed-loop transfer functions are shaped using the weighting functions W_1, W_2 and W_3.

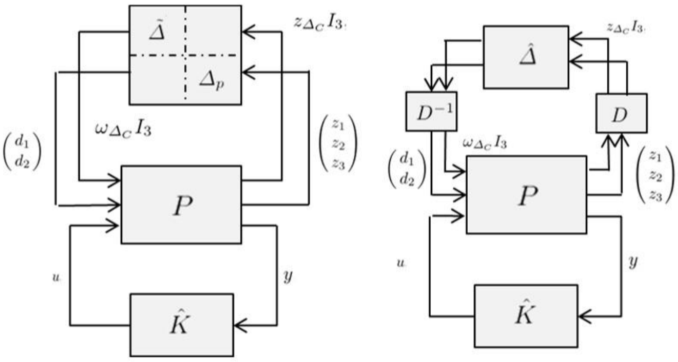

FIG.5. Closed loop interconnected design for structured μ-Synthesis

In Fig. 5 one can see the general interconnection scheme for structured μ-Synthesis where $\tilde{K} = diag(K, K, K)$ and $\tilde{\Delta} = diag(\Delta_c, \Delta_c, \Delta_c)$. Thus the block $\hat{\Delta} = diag(\tilde{\Delta}, \Delta_p)$ is constructed with the help of scaling matrices D. For that end, consider $\tilde{D}(s) = D(s) - I$ such that $\tilde{D}(j\omega)\tilde{\Delta} = \tilde{\Delta}\tilde{D}(j\omega)$ with $D(j\omega) \in \Lambda$. With the new scalings one obtains:

$$D(j\omega)F_l\left(\tilde{P}(j\omega), \tilde{K}(j\omega)\right)D^{-1}(j\omega) = F_l\left(\hat{P}(s), \begin{bmatrix} \tilde{K}(s) & 0 & 0 \\ 0 & \tilde{D}(s) & 0 \\ 0 & 0 & \tilde{D}(s) \end{bmatrix}\right). \tag{10}$$

Thus the structured μ-synthesis becomes the non-smooth program with block diagonal controller $K(s) = diag\left(\tilde{K}(s), \tilde{D}(s), \tilde{D}(s)\right)$

$$\begin{cases} \text{minimize}_{K(s)} \sup_\omega \overline{\sigma}\left(\hat{P}(s), K(s)\right) \\ K(s) := \begin{bmatrix} \tilde{K}(s) & 0 & 0 \\ 0 & \tilde{D}(s) & 0 \\ 0 & 0 & \tilde{D}(s) \end{bmatrix}, \tilde{D}(s) \in \Lambda, \end{cases} \tag{11}$$

and can be solved with the Hinfstruct function from MATLAB toolbox.

4. PERFORMANCE ANALYSIS

This chapter presents the simulation results of the above method and compares the resulted reduced order μ-Synthesis controller with the results from [7]

The controller order is chosen to be 2 and following using the procedure Hinfstruct one obtains the controller $K_\mu = [K_{1\mu}\ K_{2\mu}]$ ($K_{1\mu}$ uses $B_{K_\mu}(:,1)$, while $K_{2\mu}$ uses $B_{K_\mu}(:,2:4)$):

$$A_{K_\mu} = \begin{bmatrix} -0.6423 & -6.812 \\ 0.6387 & -110.4 \end{bmatrix};\ B_{K_\mu} = \begin{bmatrix} 0.7759 & 1.313 & 0.6676 & -0.5121 \\ 2.195 & 9.48 & 19.73 & 16.25 \end{bmatrix};$$
$$C_{K_\mu} = [-0.8693 \quad 10.97];\ D_{K_\mu} = [0.9277 \quad -0.4702 \quad -3.34 \quad -3.975]. \tag{12}$$

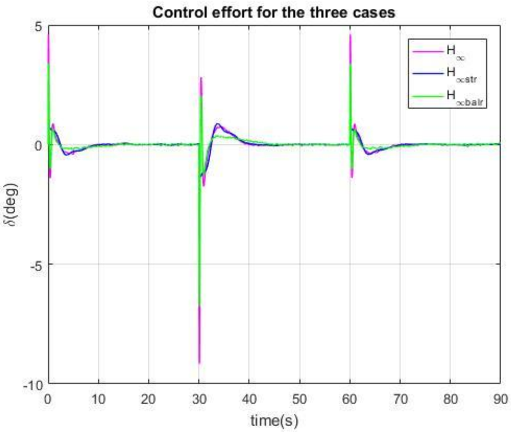

(a)

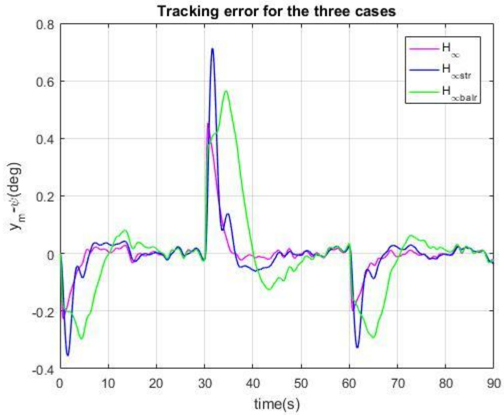

(b)

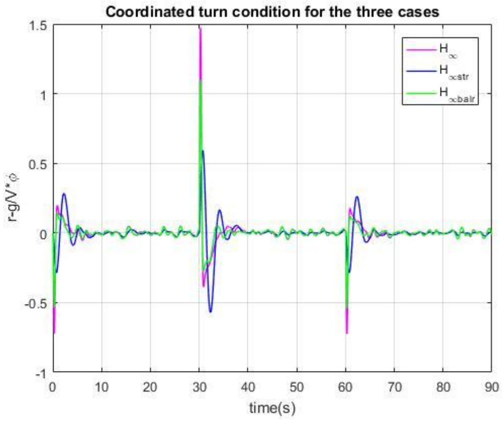

(c)

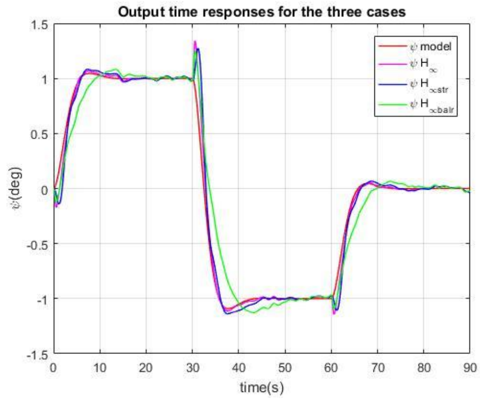

(d)

FIG.6. Performance analysis in turbulent atmosphere of HIRRUS UAV for the three proposed cases

Fig. 6 illustrates the performance analysis given by the control configuration in Fig. 2, in which the controllers $[K_1\ K_2]$ have been replaced corresponding to the three proposed controllers. The first one is the full eight-order H$_\infty$ controller (magenta line color) obtained in [7] the second one is the structured μ-Synthesis second-order controller (blue line color) obtained in (12) and the third is the reduced fifth-order H$_\infty$ controller obtained through a truncating balanced realization technique obtained also in [7] (green line color). One can see that the full order controller achieves the best tracking error Fig.6 (b,d) with respect to the reference model, while the fifth-order one has the worst tracking error. The second order controller, although it has the biggest spike at tracking error, because of the doublet type command, it recovers quicker than the fifth-order one. In terms of control deflection Fig.6 (a) the full order controller has the biggest spike of approximately 9 deg., while the second order is deflected for about 2 deg. Also one obtains the H$_\infty$ norm for the second-order controller to be $\gamma_{min} = 136.25$, while for the full eight-order one $\gamma_{min} = 76.491$. The coordinated turn requirement Fig.6 (c) in (DO3) is best achieved by the fifth order controller, closely following the full order controller, but without the spike.

CONCLUSIONS

From the performance analysis chapter one can conclude that the structured μ-Synthesis second-order controller gives better results than the fifth order one obtain through truncating the full order one. Even tough is only a second order controller it achieves good performances with respect to the full eight-order one.

AKNOWLEDGMENT

This paper has been supported by MEN-UEFISCDI, Program Partnerships, Projects PN-II-PT-PCCA- 2013-4-1349.

REFERENCES

[1] G. Stenfelt and U. Ringertz, *Lateral Stability and Control of Tailless Aircraft Configuration*, Journal of Aircraft, vol. 46, no. 6, pp. 2161-2164, 2009.

[2] A.D. Ngo, W.C. Reigelsperger and S.S. Banda, *Tailless Aircraft Control Law Design Using Dynamic Inversion and* m*-Synthesis*, Proceedings of the 1996 IEEE International Conference on Control Applications, September 15-18, 1996, Dearborn, MI, pp. 107-112, 1996.

[3] M. Voskuijl, G. La Rocca and F. Dircken, *Controllability of Blended Wing Body Aircraft*, Proceedings of the 26th International Congress of the Aeronautical Sciences (ICAS), USA, 2008.

[4] V.G. Nair, M.V. Dileep and V.I. George, Aircraft yaw control system using LQR and fuzzy logic controller, *International Journal of Computer Applications*, vol. 45, no. 9, pp. 25-30, 2012.

[5] A.-M. Stoica: L_1 *Controller Design for a Flying Wing Unmanned Aerial Vehicle*, Proceedings of ICMERA, 24-27 October 2013, Bucharest, Romania, 2013.

[6] User Guide for mini UAS Hirrus v1.2, Autonomous Flight Technology, 2015.

[7] A. M. Stoica, P. V. Parvu, M. Bivolaru, *An* H_∞ *Design Approach for the Heading Hold Autopilot of a Flying Wing UAV*, Applied Mechanics and Materials, Vol. 841, pp. 315-322, 2016

[8] A. Falcoz, C.Pittet, S.Bennani, A. Guignard, B. Frapard, *Systematic design methods of robust and structured controllers for satellite: Application to the refinement of Rosetta's orbit controller,* CEAS space journal, vol. 7, n3, pp. 319-334, 2015

[9] G. Balas, J. Doyle, K. Glover, A. Packard, R. Smith, μ*-analysis and synthesis toolbox*, MUSYN Inc. and The MathWorks Inc., Natick MA (1991)

[10] D. McLean, *Automatic Flight Control Systems*, Prentice Hall International, 1990.